Theoretical Study on Unimolecular Reactions of Acetyl Cyanide and Acetyl Isocyanide

R. Sumathi*,† and Minh Tho Nguyen*

Department of Chemistry, University of Leuven, Celestijnenlaan 200F, B-3001 Leuven, Belgium

Received: July 28, 1997; In Final Form: November 5, 1997

The potential energy surfaces of acetyl cyanide and its functional isomer acetyl isocyanide in their electronic ground state have been investigated using ab initio molecular orbital MP2(FU)/6-311G** and QCISD(T)/6-311G** calculations. The molecular eliminations of CH_3COX (X = CN,NC) to $CH_3X + CO$, $HX + CH_2CO$, and $CH_2 + HCOX$, the unimolecular rearrangements to CH_3C-OX and CH_3O-CX carbenes, 1,3-hydrogen migration to $CH_2{=}C(OH)X$, 1,3-methyl migration to CH_3NCCO, and radical decompositions to $X^{\bullet} + CH_3CO$ and $CH_3^{\bullet} + COX$ have been examined. Also the secondary decomposition processes of COCN and CONC radicals in their ground states and the secondary elimination of HX from $CH_2{=}C(OH)X$ have been investigated. Cyanide−isocyanide isomerization is found to be the predominant channel in the unimolecular reactions of acetyl cyanide. Despite being exothermic, the decomposition of acetyl cyanide into $CH_3CN + CO$ is found to be kinetically unfavorable. Decomposition into $HCN + CH_2CO$, the reverse reaction of CH_3COCN synthesis, is found to be a preferred dissociation pathway and is expected to compete at high temperatures with the 1,3-hydrogen migration, yielding cyanovinyl alcohol. The barriers for the rearrangement processes to carbenes in acetyl isocyanide are quite high in contrast to those of acetaldehyde and fluoroformaldehyde. The large magnitude of the reverse barrier from the carbenes to acetyl cyanide suggests the stability of the carbenes. In the ground state of CH_3COX, the CH_3-C bond cleavage is found to be more facile compared to the C(O)−X bond cleavage. The secondary dissociation from CONC requires a rather small barrier, and both cyanide and isocyanide forms are found to have very similar potential energy surface.

1. Introduction

Unimolecular dissociation dynamics of small polyatomic molecules have evoked considerable attention, both theoretically and experimentally. A qualitative understanding of a chemical reaction and the ability to predict the branching between the energetically allowed product channels are the points of interest in this area. Formaldehyde,[1] acetaldehyde,[2,3] acetyl chloride,[4] and fluoroformaldehyde[5] are the few prototypes of the carbonyl compounds in which photochemical and thermal dissociations, involving the ground- and excited-state surfaces, are studied extensively by both experiment and theory. Acyl cyanides are also carbonyl compounds containing, in particular, a multiply bonded substituent. Hence, their thermal and photofragmentation pathways and dynamics could well be different from those of the family of much studied carbonyl compounds containing first-row substituents. The first member of the acyl cyanides family, formyl cyanide HC(O)CN, has been synthesized[6] in 1987. Bevan et al[7a] reported a lifetime of 45.5 h, and they established the fact that HC(O)CN does not undergo a spontaneous unimolecular decomposition to HCN + CO. Theoretical calculations by Wang et al.[7b] on HC(O)CN attribute its weak stability to the facile decarbonylation giving HCN at high temperatures. However, the next member, acetyl cyanide, is thermostable[8] at ca. 350° and has been catalytically synthesized at this temperature from ketene and hydrogen cyanide. The breakdown of acetyl cyanide at ca. 470 °C was investigated by Bennett et al.[9] who found that the reaction proceeded predominantly via decarbonylation (a) as observed in formylcyanide and acetyl halides.

$$CH_3C(O)CN \rightarrow CO + CH_3CN \qquad (a)$$

However, scission to ketene and hydrogen cyanide (b) was also found to be competitive.

$$CH_3C(O)CN \rightarrow HCN + CH_2CO \qquad (b)$$

Recently, Okado and Saito[10] studied thermal unimolecular reactions of $CH_3C(O)CN$ diluted in Ar behind shock waves over the temperature range 1014−1300 K, and they have not observed CH_3CN, one of the products of decomposition (a) observed by Bennett et al.[9] These authors also performed ab initio calculations using a small split valence basis set (3-21G) and confirmed that the unimolecular decompositions are energetically less favorable compared to the isomerization to acetyl isocyanide. On the other hand, the major product of 193-nm photolysis[11] of acetyl cyanide was found to be the CN radical. The photolysis results were explained by two primary decomposition channels producing $CH_3CO + CN$ and $CH_3 + COCN$, respectively, with the first channel being predominant. Although acetyl cyanide is a very common molecule, as can be seen, very little is known of its various possible thermal and photochemical decomposition and rearrangement kinetics. To gain a better understanding of the mechanism and kinetics of its gas-phase decomposition, we carried out a detailed theoretical study, at a high level of theory, of the isomerization and decomposition channels.

In this paper, we consider the possible decomposition and rearrangement channels on the ground-state surface of both

† On leave from Manonmanium Sundaranar Univerisity, Tirunelveli-627 002, India.

S1089-5639(97)02458-4 CCC: $15.00
Published on Web 01/08/1998

SCHEME 1

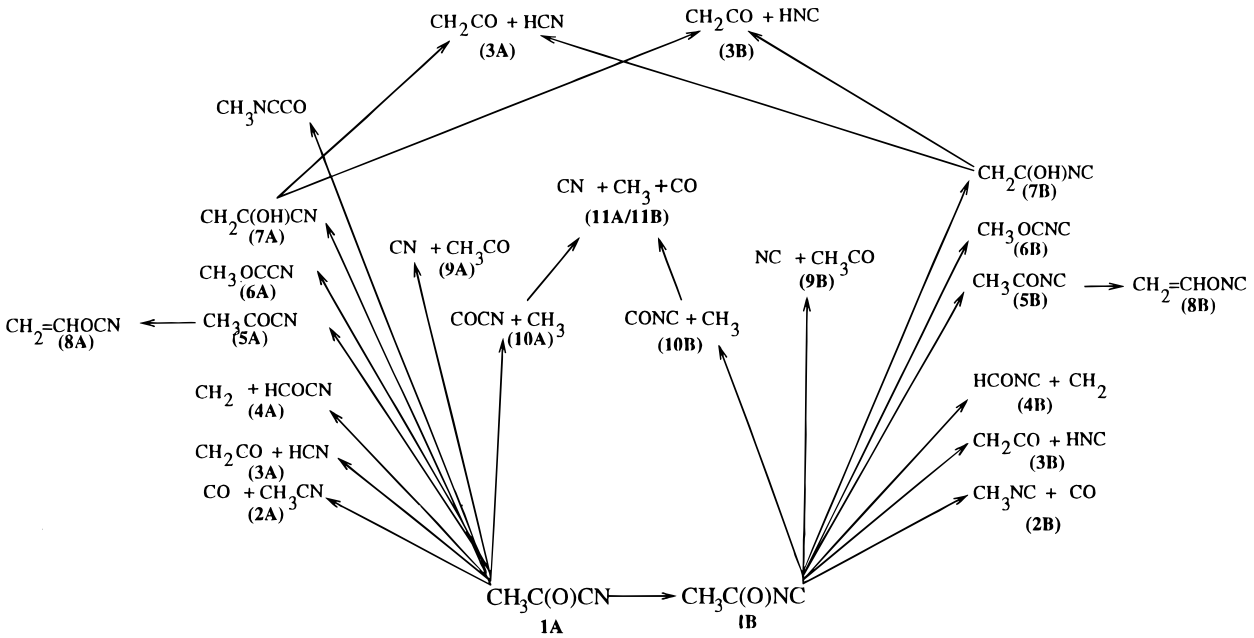

CH_3COCN and CH_3CONC. The various molecular decomposition channels are

$$CH_3C(O)CN\ (\mathbf{1A}) \rightarrow \begin{cases} CH_3CN + CO & (\mathbf{2A}) \\ HCN + CH_2CO & (\mathbf{3A}) \\ CH_2 + HCOCN & (\mathbf{4A}) \end{cases}$$

$$CH_3C(O)NC\ (\mathbf{1B}) \rightarrow \begin{cases} CH_3NC + CO & (\mathbf{2B}) \\ HNC + CH_2CO & (\mathbf{3B}) \\ CH_2 + HCONC & (\mathbf{4B}) \end{cases}$$

The various isomerization channels considered for investigation are

$$CH_3C(O)CN\ (\mathbf{1A}) \rightarrow \begin{cases} CH_3C\text{-}OCN & (\mathbf{5A}) \\ CH_3O\text{-}CCN & (\mathbf{6A}) \\ CH_2C(OH)CN & (\mathbf{7A}) \\ CH_3NCCO & (\mathbf{12A}) \end{cases}$$

$$CH_3C\text{-}OCN\ (\mathbf{5A}) \rightarrow \begin{cases} CH_2{=}CHOCN & (\mathbf{8A}) \\ CH_3C\text{-}ONC & (\mathbf{5B}) \end{cases}$$

$$CH_3C(O)NC\ (\mathbf{1B}) \rightarrow \begin{cases} CH_3O\text{-}CNC & (\mathbf{6B}) \\ CH_2C(OH)NC & (\mathbf{7B}) \end{cases}$$

$$CH_3C\text{-}ONC\ (\mathbf{5B}) \rightarrow CH_2{=}CHONC\ (\mathbf{8B})$$

in addition to $CH_3C(O)CN$ (**1A**) → CH_3CONC (**1B**) isomerization. We also examined both primary and secondary radical decomposition processes, namely,

$$CH_3C(O)CN\ (\mathbf{1A}) \rightarrow \begin{cases} CH_3CO + CN & (\mathbf{9A}) \\ CH_3 + COCN & (\mathbf{10A}) \end{cases}$$

$$CH_3C(O)NC\ (\mathbf{1B}) \rightarrow \begin{cases} CH_3CO + NC & (\mathbf{9B}) \\ CH_3 + CONC & (\mathbf{10B}) \end{cases}$$

$$C(O)CN\ (\mathbf{10A}) \rightarrow CO + CN\ (\mathbf{11A})$$

$$C(O)NC\ (\mathbf{10B}) \rightarrow CO + NC\ (\mathbf{11B})$$

arising from $CH_3C(O)CN$ and $CH_3C(O)NC$ molecules. The barriers to the unimolecular rearrangement pathways **5A**, **5B**, **6A**, and **6B** are critical to isolation of these carbene isomers. There is experimental evidence for such isomers derived from formaldehyde[12] and formyl fluoride.[13] The purpose of this work is to determine the barrier heights for the above-mentioned unimolecular dissociation and rearrangement processes. A comparison of the results has been made with the earlier ab initio results reported for the HFCO,[5] CH_3COCl,[4] CH_3CHO,[3] and HC(O)CN[7] decompositions. When this article was under preparation, we came across a recent study of So[14] on the unimolecular reactions of acetyl cyanide. In his work, So has considered a few of the channels studied here, namely, **2A**, **3A**, **5A**, **6A**, **1B**, and **2B** formation and optimized the structures at the MP2/6-31G* level and computed energies at the G2 level. They have not considered the competitive isomerization to cyanovinyl alcohol (**7A**) and its decomposition to HCN + CH_2CO and HNC + CH_2CO. Such an isomerization was found[15] to play a major role in the kinetics of acetic acid decomposition, and the ketene formation in acetic acid was found to proceed completely via the 1,1-ethenediol intermediate. Hence, we wish to present here a more complete potential energy surface comprising all possible isomerizations and dissociations starting from $CH_3C(O)CN$ and $CH_3C(O)NC$ molecules.

2. Computational Methods

All calculations were performed using the GAUSSIAN 94 program.[16] Optimized geometries were determined at the second-order perturbation theory level by taking all electrons into correlation, which we represent as MP2(FU), and by using the 6-311G** basis set. The stationary points were characterized by vibrational analysis at the MP2(FU)/6-311G** level. The unrestricted Hartree−Fock method was adopted for the open-shell systems. Single-point electronic energy calculations using QCISD(T)/6-311G** wave functions were also executed using MP2/6-311G** geometries to obtain the improved thermochemical parameters.

3. Results

All channels investigated in this study are shown in Scheme 1 along with their product numbers to facilitate the discussion.

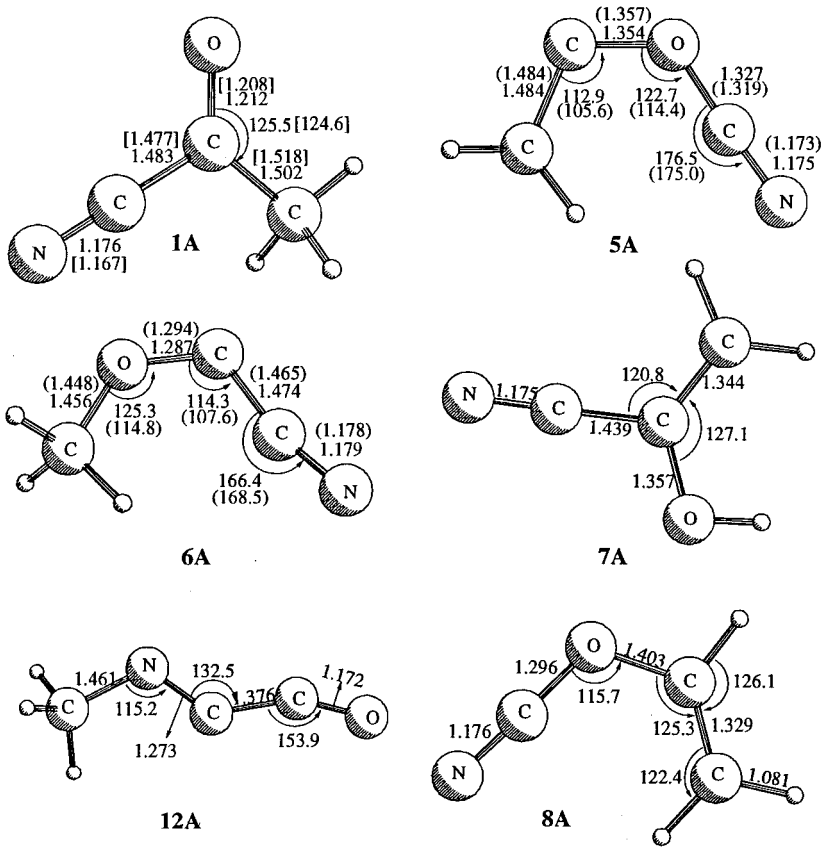

Figure 1. MP2/6-311G** optimized geometries (in Å and deg) of the equilibrium structures of acetyl cyanide (**1A**), cyanohydroxymethylcarbene (**5A**), methoxycyanocarbene (**6A**), cyanovinyl alconol (**7A**), vinyl cyano ether (**8A**), and methyliminoethanone (**12A**). Numbers in brackets and parentheses refer to the experimental values and the parameters corresponding to the trans conformers, respectively.

In general, all products arising from $CH_3C(O)CN$ are labeled **A**, and those arising from $CH_3C(O)NC$ are labeled **B**. The transition structures are numbered with both the reactant and product numbers. The MP2(FU)/6-311G** optimized geometries of acetyl cyanide (**1A**) and the unimolecular rearrangement products from acetyl cyanide, namely, cyanohydroxymethylcarbene (**5A**), methoxycyanocarbene (**6A**), cyanovinyl alcohol (**7A**), and vinyl cyano ether (**8A**), are given in Figure 1. The corresponding rearrangement products of acetyl isocyanide (**1B**), namely, isocyanohydroxymethylcarbene (**5B**), methoxyisocyanocarbene (**6B**), isocyanovinyl alcohol (**7B**), and vinyl isocyano ether (**8B**) are shown in Figure 2.

In general, **X/Y** refers to a transition structure (TS) connecting both X and Y equilibrium structures. The transition structures for the molecular decomposition (**1A/2A**, **1A/3A**, and **1A/4A**) and rearrangement (**1A/1B**, **1A/5A**, **1A/6A**, **1A/12A**, and **1A/7A**) products from **1A** are presented in Figure 3 along with **5A/8A**, while those of **1B** are shown in Figure 4. The transition structures (**7A/3A**, **7A/3B**, **7B/3A**, and **7B/3B**) for the secondary elimination of HX from $CH_2{=}C(OH)X$ are presented in Figure 5. Figures 6 and 7 graphically summarize the major findings of this work. The energies in Figures 6 and 7 are shown relative to that of acetyl cyanide (**1A**) with the zero-point vibrational energy corrections. At all other stationary points the zero-point vibrational energy corrections are made at the MP2(FU) level. Table 1 lists the heats of reaction and activation barriers for all the processes considered. The energies used in the discussion correspond to those obtained from QCISD(T)/6-311G**//MP2-(FU)/6-311G**+ZPE(MP2) calculations, unless otherwise stated. The harmonic vibrational frequencies of all the stationary points are provided as Supporting Information.

4. Discussion

The ab initio and experimental[17] bond lengths and angles of acetyl cyanide are shown in Figure 1. The theoretical bond lengths agree to a reasonable extent with microwave data. Horwitz et al.[11] have obtained a better agreement by using a much larger, 6-311G(3df,3pd), basis set. Considering the investigation on the more extended potential energy surface, we have confined ourselves to the 6-311G** basis set. The calculated molecular rotational constants for acetyl cyanide are $A = 10.132$, $B = 4.117$, and $C = 2.982$ GHz and are in good agreement with the experimental microwave data[18] of 10.243, 4.164, and 3.015 GHz. The calculated C−C bond length of 1.483 Å indicates a partial double bond character, as it is shorter than the C−C single-bond length in ethane (1.543 Å) and longer than the C=C length in ethylene (1.339 Å). All 18 normal modes of acetyl cyanide are infrared-active and they transform as 12a′ and 6a″ modes under the symmetry operations of the C_s point group. The normal mode analysis of acetyl cyanide was first carried out by Bell et al.[19] at the Hartree−Fock level. Horwitz et al.[11] have reported the frequencies of acetyl cyanide at the frozen core MP2 level with a larger 6-311G(2d,2p) basis set. In our calculations, the characteristic C≡N, C=O, and C−C stretching vibrations were calculated to occur at 2166, 1762, and 1218 cm^{-1}, respectively. Experimentally[17] the corresponding vibrations were found to absorb at 2229, 1740, and 1178 cm^{-1}, respectively.

The characteristic harmonic vibrations of acetyl isocyanide (**1B**), namely N≡C, C−N, C=O, and C−C stretches are calculated to be 2101, 1198, 1837, and 746 cm^{-1}, respectively. However, no experimental spectoscopic data on acetyl isocyanide are available for comparison. It is worthwhile mention-

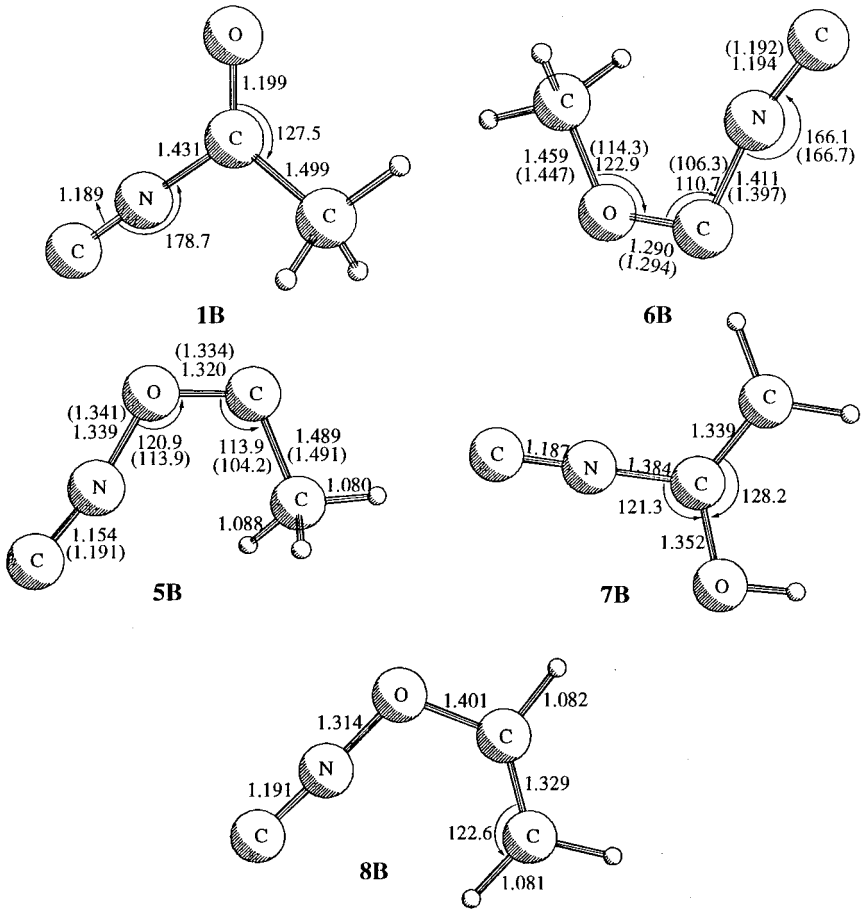

Figure 2. MP2/6-311G** optimized geometries (in Å and deg) of the equilibrium structures of acetyl isocyanide (**1B**), isocyanohydroxymethylcarbene (**5B**), methoxyisocyanocarbene (**6B**), isocyanovinyl alconol (**7B**); vinyl isocyano ether (**8B**). Numbers in parentheses refer to the trans conformer. The structure parameters of cis-**5B** are at the HF/6-31G** level.

ing that Okado and Saito in their experiments monitored the IR emission at 4.90 μm, which, from our calculations, clearly corresponds to N≡C stretching vibration (2101 cm^{-1} = 4.76 μm). Okado et al. have also reported vibrational frequencies of **1B** calculated at the Hartree−Fock level with the 3-21G basis set, and at this level, the N≡C stretching wavenumber was calculated to be 2346 cm^{-1}.

4.1. Unimolecular Rearrangements. *4.1.1. Cyanide to Isocyanide Isomerization.*

$$CH_3COCN\ (\mathbf{1A}) \rightarrow CH_3(O)NC\ (\mathbf{1B})$$

The geometry of the transition structure **1A**/**1B** has been reported at the HF/6-31G and MP2(FU)/6-31G* levels[14] and is compared with HF/3-21G results of Okado et al.[10] Since their calculated geometry of **1A**/**1B** agrees quite well with the present MP2(FU)/6-311G** value, it indicates that the geometry is insensitive to the size of the basis set, a conclusion drawn already by So.[14] The barrier for this process was found to be 40.8 kcal/mol at the G2 level, while our calculated barrier height at the QCISD(T) level is 41.3 kcal/mol. From Figures 6 and 7, it is clear that this isomerization has the lowest barrier and hence is the only reaction feasible at low temperatures. This isomerization is unique of acyl cyanides owing to its ambient cyanide substituent and is not possible in aldehydes, ketones, and acyl halides. Isomerization similar to isocyanide (HC(O)-NC) is the most favorable pathway on the HC(O)CN potential energy surface too, and it has a barrier height of 43.2 kcal/mol at the B3LYP/6-311++G** level.[20] This suggests a comparable stability for both formyl and acetyl cyanides.

4.1.2. Rearrangements to Carbenes.

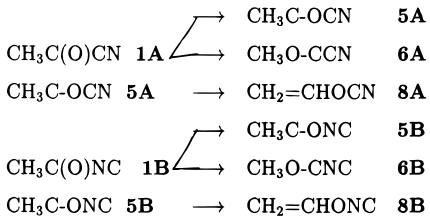

In contrast to the parent methylene (:CH_2), carbenes that contain an oxygen atom directly attached to the electron deficient carbon exhibit singlet ground electronic states. This is due to the resonance stabilizing effect of the lone pairs of electrons on the oxygen. Previous calculations on hydroxyfluorocarbene,[21,22] methoxycarbene,[23] methoxychlorocarbene,[4] and chlorohydroxymethylcarbene[4] suggest the existence of both cis and trans isomers. We have analyzed the cis and trans isomers of cyanohydroxymethylcarbene (**5A**), methoxycyanocarbene (**6A**), isocyanohydroxymethyl carbene (**5B**), and methoxyisocyanocarbene (**6B**) as well as the transition states connecting the cis and trans isomers. The cis−trans isomerization transition states are not given here. The barriers for cis−trans isomerization of methoxycyanocarbene (**6A**) and methoxyisocyanocarbene (**6B**) are 26.9 and 27.3 kcal/mol, respectively. A barrier of 27.5 kcal/mol for cis to trans rotation in hydroxymethylene has been reported.[24] The transition-state structures for internal rotations between the cis and trans forms of singlet methylene isomers have their torsional angles very close to 90°. The large barriers to these rotations arise no doubt from the partial double-bond

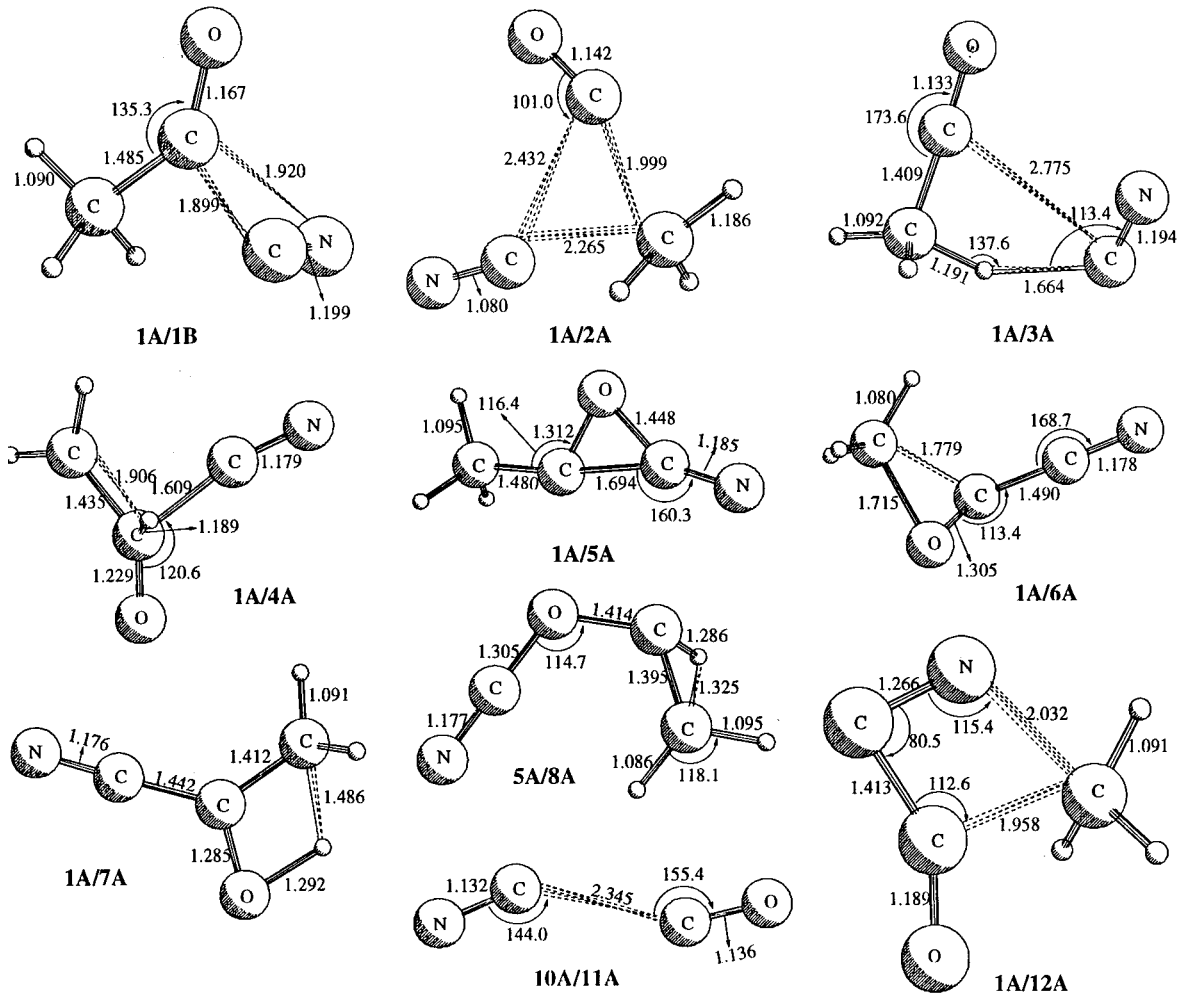

Figure 3. MP2/6-311G** optimized geometries (in Å and deg) of the transition structures **1A/1B**, **1A/2A**, **1A/3A**, **1A/4A**, **1A/5A**, **1A/6A**, **1A/7A**, **1A/12A**, **5A/8A**, and **10A/11A** on the $CH_3C(O)CN$ potential energy surface.

character of the CO bond in all cases. As the trans and cis isomers of CH_3C-OX and CH_3O-CX lie within 5 kcal/mol of each other, these internal rotation processes are nearly thermoneutral. The trans isomers of CH_3C-OCN (**5A**) and CH_3O-CCN (**6A**) are given at the MP2(FU)/6-31G* level in ref 14. All our attempts in obtaining the cis form of **5B** at the MP2 level have proved futile. In Figure 2 we have given the HF/6-31G** structure parameter values for *cis*-**5B**. The C≡N and N≡C bond lengths in carbenes are the same as in **1A** and **1B**. The carbenes **5A** and **6A** could be derived from acetyl cyanide via 1,2-migration of cyanide and methyl groups, respectively. But the barriers to produce these two carbenes from acetyl cyanide are very high (see Figures 6 and 7). It is also interesting to note that these carbenes have sufficient stability owing to its reverse barrier for the formation of acetyl cyanide. Because of their stability, they can undergo other rearrangements (for, for example **5A** to **8A** and **5B** to **8B**) to give the equally stable functional isomers of acetyl cyanide, namely, vinyl cyano ether (**8A**), and acetyl isocyanide, namely, vinyl isocyano ether (**8B**). Singlet trans CH_3OCCN (**6A**) and CH_3OCNC (**6B**) have a XCO (X = CN, NC) bond angle of 104°, typical of a singlet carbene which opens up by 7° in the cis form. The C−O distance of 1.29 Å in **6A** and **6B** reflects the partial double bond character.

The MP2(FU)/6-311G** geometries of the transition state **1A**/**5A** for 1:2 cyanide migration and **1A**/**6A** for 1:2 methyl migration are shown in Figure 3. The three-membered tight structure of **1A**/**5A** is characterized by C−C elongation (1.69 Å) and O−CN compression (1.45 Å). Analysis of the eigenvectors corresponding to the negative eigenvalue of the force constant matrix suggests the reaction coordinate as O−C−CN bending motion. The corresponding transition states from **1B**, namely, **1B**/**5B** and **1B**/**6B**, are shown in Figure 4. As can be seen, **1B**/**5B** is very similar to **1A**/**5A** and the C−N bond has increased by 0.14 Å from that of **1B**.

On the contrary, the 1,2-migration of the methyl group in **1A** and **1B** proceeds via the relatively loose transition states **1A**/**6A** and **1B**/**6B**. In the former, the migrating methyl group is 1.82 Å away from the migrating origin and 1.75 Å away from the migrating terminus. Energetically **6A** is more stable than **5A**; however, the barrier for its formation is higher than that of **5A**. This is expected from the fact that **5A** results via the cleavage of the highly delocalized OC−CN bond, in other words, a partial double bond. On the other hand, **6A** arises because of migration of a methyl group, which is singly bonded to the C(O)CN fragment. Both the transition structures are below the $CH_3CO + CN$ radical dissociation limit and lie above the $CH_3 + COCN$ limit (Figure 6), and hence they can hardly compete with the radical dissociations at higher temperatures. Moreover, the frequency factors for radical dissociations are generally higher than that for isomerization, and hence at higher temperatures the system would prefer to undergo dissociation than rearrangement. Nevertheless, the carbenes, if formed, are expected to be stable owing to their large reverse barrier to cyanide formation.

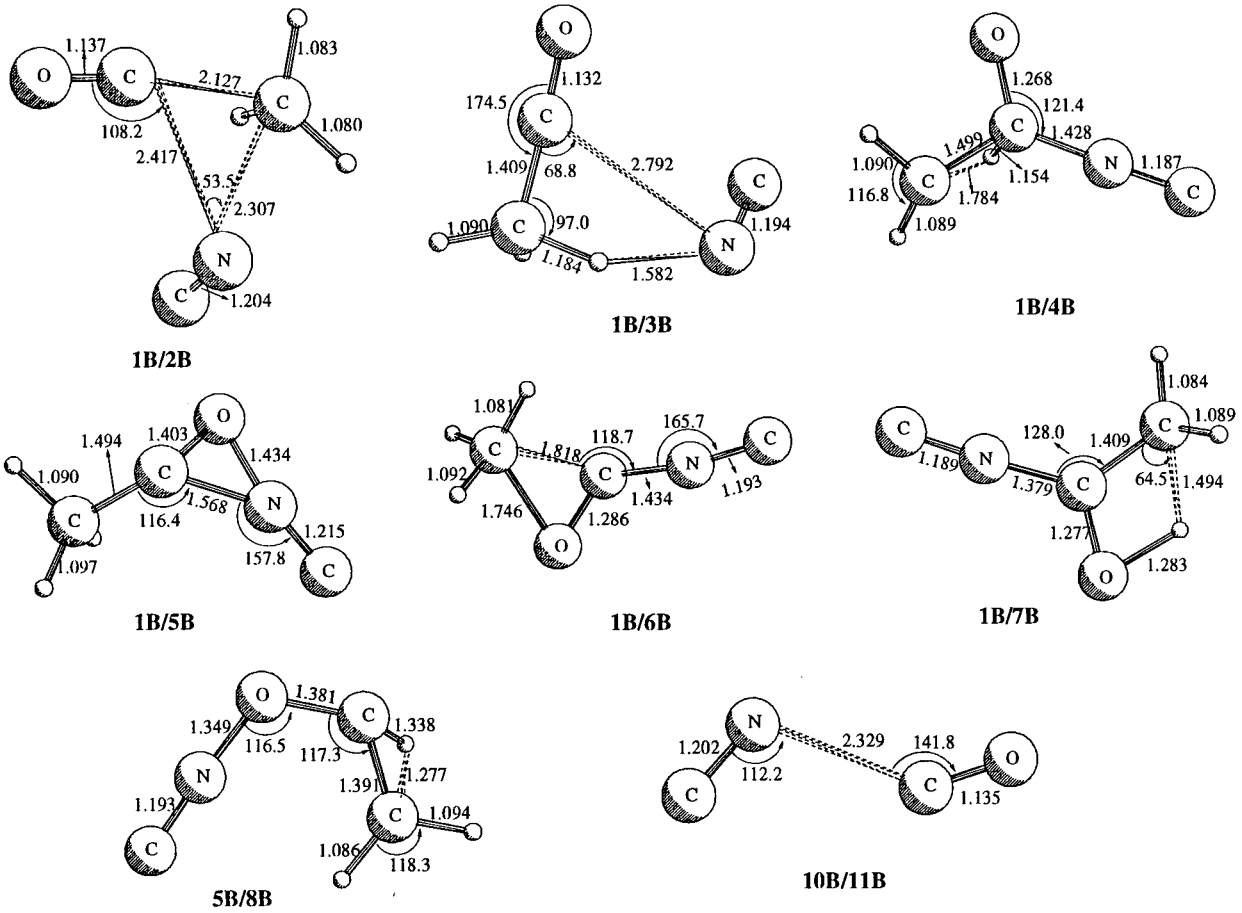

Figure 4. MP2/6-311G** optimized geometries (in Å and deg) of the transition structures **1B/2B**, **1B/3B**, **1B/4B**, **1B/5B**, **1B/6B**, **1B/7B**, **5B/8B**, and **10B/11B** on the $CH_3C(O)NC$ potential energy surface.

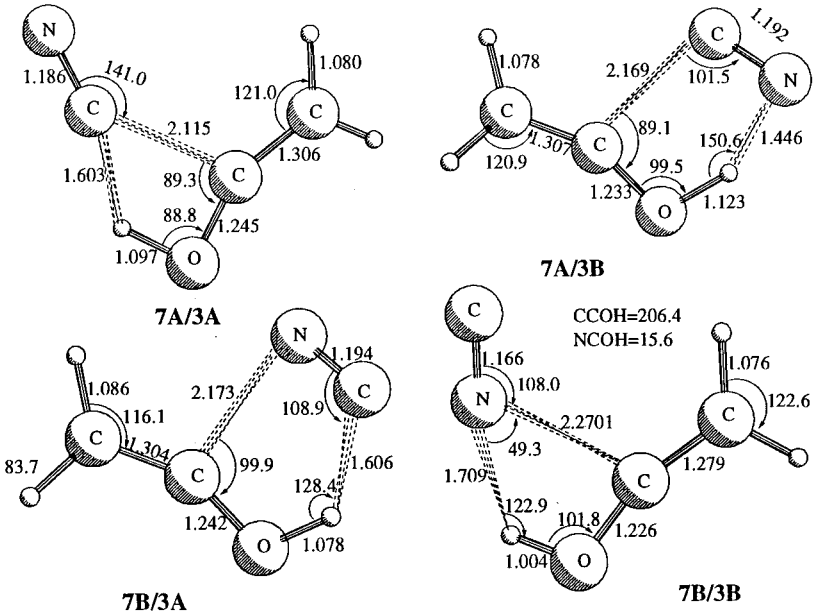

Figure 5. MP2/6-311G** optimized geometries (in Å and deg) of the transition structures **7A/3A**, **7A/3B**, **7B/3B**, and **7B/3A** on the $CH_3C(O)CN$ potential energy surface.

The 1,2-migration of hydrogen in **5A** and **5B** yields respectively the vinyl cyano ether (**8A**) and the vinyl isocyano ether (**8B**), the functional isomers of acetyl cyanide. The transition state for these reactions, **5A**/**8A** and **5B**/**8B**, are given respectively in Figures 3 and 4. The carbene **5A** will easily undergo isomerization to vinyl cyano ether (**8A**) rather than to acetylcyanide owing to its low barrier height.

4.1.3. Rearrangement to Cyano and Isocyanovinyl Alcohol.

$$CH_3C(O)CN\ (\mathbf{1A}) \rightarrow CH_2C(OH)CN\ (\mathbf{7A})$$

$$CH_3C(O)NC\ (\mathbf{1B}) \rightarrow CH_2C(OH)NC\ (\mathbf{7B})$$

Another important unimolecular isomerization is the 1,3-hydrogen migration from the methyl group to the carbonyl

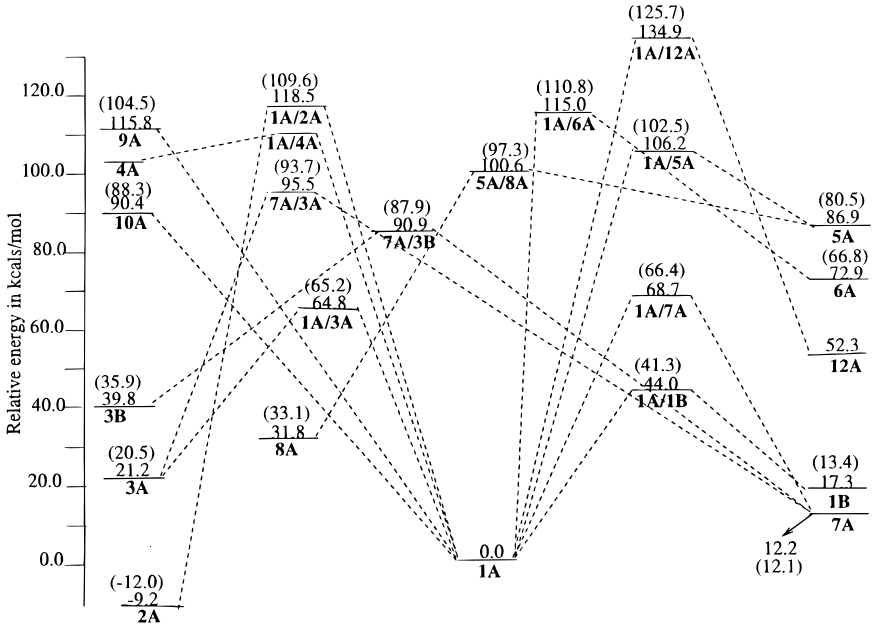

Figure 6. Overall profile of the potential energy surface for the $CH_3C(O)CN$ molecule calculated at the MP2/6-311G** and QCISD(T)/6-311G**//MP2/6-311G** levels. Numbers in parentheses refer to the QCISD(T) level.

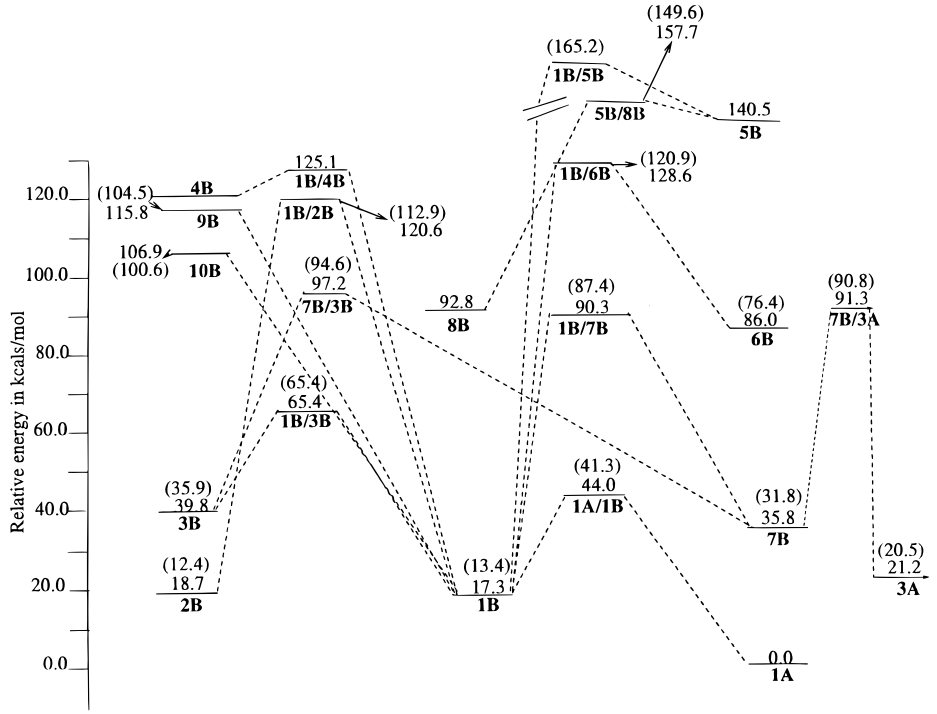

Figure 7. Overall profile of potential energy surface for the $CH_3C(O)NC$ molecule calculated at the MP2/6-311G** and QCISD(T)/6-311G**//MP2/6-311G ** levels. Numbers in parentheses refer to the QCISD(T) level.

oxygen of the acetyl cyanide, giving rise to vinyl derivatives. Thermodynamically this reaction is less endothermic compared to other unimolecular rearrangement processes. This channel has not been considered by So[14] in his investigation, and such a channel has not been investigated in the unimolecular reactions of acetylchloride.[4] As mentioned in the Introduction, this channel was found to play an important role in acetic acid decomposition,[15] and hence it is necessary to establish the significance of this process in the reaction dynamics of acyl cyanides. Transition structure searches for hydrogen migration from carbon to oxygen located a transition state **1A/7A**. The isomerization transition state, **1A/7A**, as shown in Figure 3, is a four-membered transition state, and all four atoms lie approximately in the same plane. The migrating hydrogen is 1.29 and 1.49 Å, respectively, away from the migrating origin and terminus. The reaction coordinate has been identified as the asymmetric C···H−O stretch, and the magnitude of the vibration which has been lost at the transition state is 2359i cm^{-1}. The transition structure is only 66.4 kcal/mol higher than **1A/1B** and is almost of the same energy as **1A/3A** (discussed in the next section), suggesting it as a competing channel to process **3A**. Although the barriers are very close, the importance of this channel depends on the magnitude of its preexponential factor as compared to that of the molecular dissociation channel

TABLE 1: Calculated Heats of Reaction and Energy Barriers in kcal/mol at Both the MP2(FU) and QCISD(T) Levels with the 6-311G Basis Set and Based on MP2 Geometries**

	heats of reaction		energy barriers	
reaction	MP2	QCISD(T)	MP2	QCISD(T)
$CH_3C(O)CN \rightarrow CH_3C(O)NC$ (**1B**)	17.3	13.4	44.0	41.3
$CH_3C(O)CN \rightarrow CH_3CN + CO$ (**2A**)	−9.2	−12.0	118.5	109.6
$CH_3C(O)CN \rightarrow HCN + CH_2CO$ (**3A**)	21.2	20.5	64.8	65.2
$CH_3C(O)CN \rightarrow CH_2 + HCOCN$ (**4A**)	102.8	101.9	110.2	102.7
$CH_3C(O)CN \rightarrow CH_3C-OCN$ (**5A**)	86.9	80.5	106.2	102.5
$CH_3C(O)CN \rightarrow CH_3O-CCN$ (**6A**)	72.9	66.8	115.0	110.8
$CH_3C(O)CN \rightarrow CH_2C(OH)(CN)$ (**7A**)	12.2	12.1	68.7	66.4
$CH_3C(O)CN \rightarrow CH_3CO + CN$ (**9A**)	115.8	104.5	115.8	104.5
$CH_3C(O)CN \rightarrow CH_3 + COCN$ (**10A**)	90.4	88.3	90.4	88.3
$CH_3C-OCN \rightarrow CH_2{=}CHOCN$ (**8A**)	55.1	47.4	13.7	16.8
$CH_3C(O)NC \rightarrow CH_3NC + CO$ (**2B**)	1.4	1.0	103.3	99.5
$CH_3C(O)NC \rightarrow HNC + CH_2CO$ (**3B**)	22.5	22.5	48.1	52.0
$CH_3C(O)NC \rightarrow CH_2 + HCONC$ (**4B**)	102.6	91.4	107.8	101.4
$CH_3C(O)NC \rightarrow CH_3C-ONC$ (**5B**)	123.2	127.8	155.6	151.8
$CH_3C(O)NC \rightarrow CH_3O-CNC$ (**6B**)	68.7	63.0	111.3	107.5
$CH_3C(O)NC \rightarrow CH_2C(OH)(NC)$ (**7B**)	18.5	18.4	73.0	74.0
$CH_3C(O)NC \rightarrow CH_3CO + NC$ (**9B**)	98.5	91.1	98.5	91.1
$CH_3C(O)NC \rightarrow CONC + CH_3$ (**10B**)	89.6	93.5	89.6	93.5
$CONC \rightarrow CO + NC$ (**11B**)	13.5	7.5	30.1	12.5

(**3A**). Hence we have computed the preexponential factors for both the processes as

$$A_i = \frac{k_B T}{h} \frac{Q^{\dagger}}{Q}$$

where k_B is the Boltzmann constant, h is Planck's constant, T is the temperature in Kelvin, and $Q_i^{\dagger}$ and Q_i are the complete partition functions for the respective transition state and the reactant, respectively. The partition functions were obtained from the MP2 level calculated harmonic vibrational frequencies and moments of inertia. The frequency factor at 300 K for processes **3A** and **8A** are 4.0×10^{12} and 2.58×10^{12} s^{-1}, respectively. These results indicate that at lower temperatures acetyl cyanide preferentially undergoes isomerization to acetyl isocyanide, while at high temperatures the formation of both cyanovinyl alcohol and HCN + CH_2CO products are equally favorable, an important conclusion derived from our more complete PES. Experimentally, it should be possible to observe vibrations at OH stretching frequencies during the high-temperature thermal decomposition of acetyl cyanide.

On the contrary, the barrier for 1,3-hydrogen migration in acetyl isocyanide is quite high, 87.4 kcal/mol, compared to HNC + CH_2CO products. From Figure 7, it is clear that acetyl isocyanide undergoes preferential isomerization to cyanide at low temperatures and dissociates into HNC + CH_2CO at higher temperatures.

It is appropriate to mention that in acetic acid, the corresponding 1,3-hydrogen migration was found[15] to have a lower barrier (74.3 kcal/mol) than its dissociation (75.8 kcal/mol) into ketene and water. Also the secondary dehydration (second step) involves

$$CH_3COOH \rightarrow CH_2{=}C(OH)_2 \rightarrow CH_2CO + H_2O$$

an energy barrier of only 74.6 kcal/mol. Consequently, these authors have shown from their detailed kinetic analysis that ketene formation from acetic acid is a two-step process and it involves the 1,3-hydrogen migration product 1,1-ethenediol as the primary intermediate. The presense of a cyanide group, however, leads to a slight preference for process **3A** over **7A**. Nevertheless, it may be possible for $CH_2C(OH)X$ to be an intermediate in HX formation at high temperatures provided the secondary elimination barrier for HX formation from **7A** is lower than the barrier for its formation from acetyl cyanide, Hence, we have investigated both the 1,2-hydrogen and 1,3-hydrogen migrations from **7A** and **7B**,

$CH_2C(OH)CN$ **7A** → HCN + CH_2CO **3A**
$CH_2C(OH)CN$ **7A** → HNC + CH_2CO **3B**
$CH_2C(OH)NC$ **7B** → HCN + CH_2CO **3A**
$CH_2C(OH)NC$ **7B** → HNC + CH_2CO **3B**

and the corresponding four- and five-membered transition structures are shown in Figure 5. Both the migrations are associated with a simultaneous cleavage of the C(OH)−X bond, and the transition structures are highly nonplanar. As can be seen from Figures 6 and 7, in contrast to the acetic acid system, these pathways (second step) involve substantially higher barriers compared to the first step. In general, the probability for the reaction decreases with an increasing number of intermediates, and it decreases still further when the energetics of the second step are unfavorable. Hence, we conclude that the HX formation in acetyl cyanide occurs preferentially by the one-step molecular dissociation channel.

4.1.4. Rearrangement to Methyliminoethanone.

$$CH_3C(O)CN\ (\mathbf{1A}) \rightarrow CH_3NCCO\ (\mathbf{12A})$$

Our calculations on the molecular dissociation channels (discussed in the next section) indicate that dissociation of **1A** into CH_3NC + CO via its isomerization to **1B** is kinetically unfavored. We could not locate the transition state for the single-step decomposition of **1A** to **2B**. So[14] has also expressed his inability to obtain such a transition state. Hence we wish to probe the other pathways for its formation. In this regard, the work by Flemming et al.[25] shows that methyliminoethanone requires only 7.9 kJ/mol for its dissociation into CH_3NC and CO. Therefore, it is of necessity to investigate the barrier height for CH_3NCCO formation from **1A**. Hence, we studied the 1,3-methyl migration in acetylcyanide yielding the imino-substituted heterocumulenes, CH_3NCCO. 1,3-Methyl migration is an endothermic (52.5 kcal/mol) process, and it, however, involves a large barrier height of 134.8 kcal/mol. Hence, this process is unlikely to contribute in the reaction kinetics of acylcyanides. Also it is clear from our extensive calculations that decar-

bonylation yielding CH_3X from acyl cyanides is a highly unfavorable process. Both the single step and multistep decarbonylation routes, namely

$$CH_3C(O)CN \rightarrow CH_3CN + CO \ (\mathbf{2A})$$

$$CH_3C(O)CN \rightarrow CH_3NC + CO \ (\mathbf{2B})$$

$$CH_3C(O)CN \rightarrow CH_3C(O)NC \rightarrow CH_3NC + CO \ (\mathbf{2B})$$

$$CH_3C(O)CN \rightarrow CH_3NCCO \rightarrow CH_3NC + CO \ (\mathbf{2B})$$

are accompanied by barriers that lie above the radical dissociation limits. The structure of the transition state **1A/12A** is given in Figure 3 for completion.

4.2. Molecular Dissociation Pathways. Let us first examine the following dissociations:

$CH_3C(O)CN$ **1A** → $CH_3CN + CO$ **2A**
→ $HCN + CH_2CO$ **3A**
→ $CH_2 + HCOCN$ **4A**

$CH_3C(O)NC$ **1B** → $CH_3NC + CO$ **2B**
→ $HNC + CH_2CO$ **3B**
→ $CH_2 + HCONC$ **4B**

All the six molecular dissociation processes (i.e., **2A**, **3A**, **4A**, **2B**, **3B**, **4B**) except **2A** are endothermic (Table 1). The relevant activation barriers are substantial and lie above the $CH_3CO + CN$ dissociation limits for the processes **2A**, **2B**, and **4B**. Although the process **2A** is exothermic by 12.0 kcal/mol, it is kinetically unfavored owing to its large barrier of 109.6 kcal/mol. This is similar to the case of CH_3COCl[4] and HCOCN[7] and is in line with the experimental observation of Okada and Saito.[10]

The transition structure **1A/2A** maintains a C_s symmetry and involves a loose three-membered ring. The C−CN distance of 2.43 Å is long relative to the C−CN distance of 1.48 Å in acetyl cyanide. The C═O distance of 1.14 Å is closer to its value in product carbon monoxide (1.14 Å) as compared to reactant acetyl cyanide (1.21 Å). The imaginary frequency of 921.5i cm^{-1} mainly involves a CCC bending motion. A qualitatively similar transition structure (C_s symmetry) has been observed for dissociation of acetaldehyde[3] to CH_4 and CO, acetyl chloride[4] to CH_3Cl and CO, and formamide[26] to NH_3 and CO.

A similar transition structure has been found for the formation of methyl isocyanide from CH_3CONC (**1B**). The **1B/2B** also involves a loose three-membered ring with elongated C−CO (2.13 Å) and C−NC (2.31 Å) bonds. The N−C bond length in the NC fragment has increased by 0.01 Å from the reactant. Both the decomposition processes **2A** and **2B** are kinetically controlled and are unfavored at low temperatures due to their very large barrier height.

For both acetyl cyanide (**1A**) and acetyl isocyanide (**1B**), the easiest molecular dissociation channel is 1,2-elimination of HCN or HNC along with the formation of ketene CH_2CO. This decomposition channel is the reverse reaction of cyanide synthesis. This activation barrier is 65.2 kcal/mol. The transition state **1A/3A** is of C_1 point group and the nitrogen of CN group is almost perpendicular to the loose four-membered ring. So[14] reported a C_s transition state for this process. The C−CN distance of 2.77 Å is very long relative to the distance of 1.43 Å in acetyl cyanide. The H···CN distance of 1.66 Å is also large compared to that in the equilibrium structure of HCN (1.07 Å) and is suggestive of strong vibrational excitation in the nascent HCN molecule. Since the detaching hydrogen is only 1.19 Å away from the methyl carbon, it suggests that the extent of breaking of both the C−CN and C−H bonds is not the same at the transition state. First, the CN fragment gets detached from the carbonyl carbon and then forms the bond with hydrogen. A glance at Figure 3 and Figure 4 reveals that both **1A/3A** and **1B/3B** are very similar with very similar structure parameter values. This implies that the behavior of acyl isocyanides except for their intrinsic higher energies is not much different from that of acyl cyanides.

The least preferred molecular dissociation pathway is the 1,2-hydrogen shift process to yield singlet CH_2 and HCOCN. The activation energy is estimated at 102.7 kcal/mol. The transition structure **1A/4A** is nonplanar with the migrating hydrogen atom almost bonded to the carbonyl carbon (1.19 Å). The reaction coordinate involves the movement of the CN fragment too, and the C−CN distance in **1A/4A** (1.61 Å) is larger than the corresponding distance in the product HCOCN (1.47 Å) or the reactant acetyl cyanide. The reaction is highly endothermic. The reverse reaction corresponds to an insertion of singlet methylene to the C−H bond and is thus highly exothermic and implies a small energy barrier.

The transition state **1B/4B** is relatively tighter compared to **1A/4A**, and it does not involve any movement of the NC fragment. The reaction coordinate corresponds to an asymmetric stretch of C← →H···C← as indicated by the eigenvectors of the imaginary frequency. The reaction is also highly endothermic, and the **1B/4B** is close to the products in accordance with Hammond's postulate. In summary, among the molecular decomposition pathways, the pathway leading to ketene is the most preferred one, and the HX (X = CN or NC) thus produced will be a vibrationally hot molecule.

4.3. Simple Bond Cleavages.

$CH_3C(O)CN$ **1A** → $CH_3CO + CN$ **9A**
→ $CH_3 + COCN$ **10A**

$CH_3C(O)NC$ **1B** → $CH_3CO + NC$ **9B**
→ $CH_3 + CONC$ **10B**

$C(O)CN$ **10A** → $CO + CN$ **11A**

$C(O)NC$ **10B** → $CO + NC$ **11B**

Here we are concerned with the simple homolytic bond cleavages of $CH_3C(O)CN$ and $CH_3C(O)NC$ and the secondary decomposition pathways of COCN and CONC. For radical species we adopted the UHF wave functions with the MP2 correction. The lowest bond fission reaction is the cleavage of the C−C(O)X (X = CN, NC) single bond. More energy (104.5 kcal/mol) is required to dissociate the C(O)−X, the partial double bond. The C−C bond energy is higher than the C−X bond energy in CH_3COX due to its partial double bond character. Successive bond fission of CH_3CO, •COCN, and •CONC may have barriers. Photodissociation of acetyl cyanide yields CN radicals, and these CN radicals are thought to be arising predominantly from the primary C−C dissociation channel. Investigations on the lowest excited singlet and triplet states of acetyl cyanide to probe its photodissociation dynamics are under progress. Though it is not possible to predict the barrier heights for the C−C and C−X dissociations on the excited singlet or triplet surface of CH_3COX from our ground-state calculations, we can give an estimate about the secondary dissociation barrier heights. For the decomposition channel of CH_3CO• a barrier of 18 kcal/mol has been estimated[4] earlier by us, and the transition-state structure has been given elsewhere.[4]

The structure of transition states **10A**/**11A** and **10B**/**11B** are very close to the products, and the barrier height for the CONC radical is about 12 kcal/mol.

5. Conclusions

Unimolecular isomerization to acetyl isocyanide from acetyl cyanide is the most favorable thermal process and is in accord with the experimental observations of Okado et al. However, it involves an energy barrier of 41.3 kcal/mol, which accounts for the thermal stability of acetyl cyanide. The fact that the correponding barrier height in formyl cyanide is also around 43 kcal/mol[20] suggests it to be equally as stable as acetyl cyanide. The lower well depth of acetyl isocyanide (∼27.9 kcal/mol) indicates that the isomerization is a reversible process and the equilibrium is more toward acetyl cyanide. The single-step unimolecular dissociation of **1A** into HCN and ketene has an activation barrier around ∼65 kcal/mol and is expected to contribute in the unimolecular dissociation kinetics of $CH_3C(O)X$ at high temperatures along with the 1,3-hydrogen migration channel yielding substituted vinyl alcohols. Our investigations on the multistep processes for HX formation in 1A, namely,

$$\mathbf{1A \rightarrow 7A \rightarrow 3A}$$

$$\mathbf{1A \rightarrow 7A \rightarrow 3B}$$

$$\mathbf{1A \rightarrow 1B \rightarrow 3B}$$

$$\mathbf{1A \rightarrow 1B \rightarrow 7B \rightarrow 3A}$$

$$\mathbf{1A \rightarrow 1B \rightarrow 7B \rightarrow 3B}$$

reveal that, in contrast to acetic acid system, the vinyl alcohols are not the intermediates for HX formation. Decarbonylation is a kinetically unfavored reaction either with or without an intermediate, and hence, it has no role in the thermal decomposition kinetics of acyl cyanides. The *trans*- and *cis*-methoxycyanocarbene lie at relatively low energy (≈67 kcal/mol) and may be accessible by 1,2-methyl shift. But the barrier for 1,2-methyl shift on the S_o surface is very high, making it inaccessible via a unimolecular rearrangement. The reverse barrier for the rearrangement of carbenes to CH_3COX is also quite significant, thereby suggesting a possible stability of the rearranged carbenes. On the ground-state surface, radical dissociations are direct destabilization processes and are expected to compete only at very high temperatures.

Acknowledgment. We are indebted to the Fund for Scientific Research (FWO-Vlaanderen) and Geconceerteerde Onderzoeksakties (GOA) for financial support and to the KU Leuven Computer center for providing computer facilities.

Supporting Information Available: Harmonic vibration frequencies of all stationary points (3 pages). Ordering information is available on any current masthead page.

References and Notes

(1) (a) Moore, C. B.; Weisshaar, J. C. *Annu. Rev. Phys. Chem.* **1983**, *34*, 525. (b) Chuang, M.-C.; Foltz, M. F.; Moore, C. B. *J. Chem. Phys.* **1987**, *87*, 3855 and references cited therein. (c) Scuseria, G. E.; Schaefer, H. F. *J. Chem. Phys.* **1989**, *90*, 3629.

(2) (a) Horowitz, A.; Kershner, C. J.; Calvert, J. G. *J. Phys. Chem.* **1982**, *86*, 3094. (b) Horowitz, A.; Calvert, J. G. *J. Phys. Chem.* **1982**, *86*, 3105.

(3) (a) Smith, B. J.; Nguyen, M. T.; Bouma, W. J.; Radom, L. *J. Am. Chem. Soc.* **1991**, *113*, 6452. (b) Yadav, J. S.; Goddard J. D. *J. Chem. Phys.* **1986**, *84*, 2682.

(4) (a) Sumathi, R.; Chandra, A. K. *J. Chem. Phys.* **1993**, *99*, 6531. (b) Sumathi, R.; Chandra, A. K. *Chem. Phys.* **1994**, *181*, 73. (c) Person, M. D.; Kash, P. W.; Butler, L. J. *J. Phys. Chem.* **1992**, *96*, 2021. (d) Person, M. D.; Kash, P. W.; Butler, L. J. *J. Chem. Phys.* **1992**, *97*, 355.

(5) (a) Sumathi, R.; Chandra, A. K. *Chem. Phys.* **1992**, *165*, 257. (b) Weiner, B. R.; Rosenfeld, R. N. *J. Phys. Chem.* **1988**, *92*, 4640. (c) Choi, Y. S.; Moore, C. B. *J. Chem. Phys.* **1989**, *90*, 3875. (d) Klimek, D. E.; Berry, M. J. *Chem. Phys. Lett.* **1973**, *20*, 141. (e) Morokuma, K.; Kato, S.; Hirao, K. *J. Chem. Phys.* **1980**, *72*, 1800.

(6) Judge, R. H.; Moule, D. C.; Biernacki, A.; Benkel, M.; Ross. J. M.; Rustenburg, J. *J. Mol. Spectrosc.* **1986**, *116*, 364.

(7) (a) Lewis-Bevan, W.; Gaston, R. D.; Tyrell, J.; Stork, W. D.; Salmon, G. L. *J. Am. Chem. Soc.* **1992**, *114*, 1933 and references cited therein. (b) Fang, W. H.; Liu, R. Z.; You, X. Z. *Chem. Phys. Lett.* **1994**, *226*, 453. (c) Chang, N. Y.; Yu, C. H. *Chem. Phys. Lett.* **1995**, *242*, 232. (d) Flammang, R.; Haverbeke, Y. V.; Laurent, S.; Flammang, M. B.; Wong, M. W.; Wentrup, C. *J. Phys. Chem.* **1994**, *98*, 5801.

(8) Ray, U.S. Patent 2,396,201, 1946; cf. Gresham, B.P. 583,646, 1946.

(9) Bennett, R. N.; Jones, E.; Ritchie, P. D. *J. Chem. Soc.* **1956**, 2628.

(10) Okada, K.; Saito, K. *J. Phys. Chem.* **1995**, *99*, 13168.

(11) Horwitz, R. J.; Francisco, J. S.; Guest, J. A. *J. Phys. Chem.* **1997**, *101*, 1231.

(12) (a) Sodeau, J. R.; Lee, E. K. C. *Chem. Phys. Lett.* **1978**, *57*, 71. (b) Ahmed, S. N.; Mckee, M. L.; Shevlin, P. B. *J. Am. Chem. Soc.* **1985**, *107*, 1320.

(13) Sulzle, D.; Drewello, T.; van Baar, B. L. M.; Schwarz, H. *J. Am. Chem. Soc.* **1988**, *110*, 8330.

(14) So, S. P. *Chem. Phys. Lett.* **1997**, *270*, 363.

(15) (a) Nguyen, M. T.; Sengupta, D.; Raspoet, G.; Vanquickenborne, L. G. *J. Phys. Chem.* **1995**, *99*, 11883. (b) Duan, X.; Page, M. *J. Am. Chem. Soc.* **1995**, *117*, 5114. (c) Butkovskaya, N. I.; Manke, G.; Setser, D. W. *J. Phys. Chem.* **1995**, *99*, 11115.

(16) Frisch, M. J.; Trucks, G. W.; Gordon, M. H.; Gill, P. M. W.; Wong, M. W.; Foresman, J. B.; Johnson, B. G.; Schlegel, H. B.; Robb, M. A.; Replogle, E. S.; Gomperts, R.; Andres, J. L.; Raghavachari, K.; Binkley, J. S.; Gonzalez, C.; Martin, R. J.; Fox, D. J.; Defrees, B. J.; Baker, J.; Stewart, J. J. P.; Pople, J. A. *Gaussian 94*; Gaussian Inc.: Pittsburgh, PA, 1994.

(17) Sugie, M.; Kuchitsu, K. *J. Mol. Struct.* **1974**, *20*, 437.

(18) Krisher, L. C.; Wilson, E. B. *J. Chem. Phys.* **1959**, *31*, 882.

(19) Bell, S.; Guirgis, G. A.; Lin, J.; Durig, J. R. *J. Mol. Struct.* **1990**, *238*, 183.

(20) Sengupta, D.; Peeters, J.; Nguyen, M. T. *Chem. Phys. Lett.*, in press.

(21) Goddard, J. D.; Schaefer, H. F. *J. Chem. Phys.* **1990**, *93*, 4907.

(22) Kamiya, K.; Morokuma, K. *J. Chem. Phys.* **1991**, *94*, 7287.

(23) Yadav, J. S.; Goddard, J. D. *J. Chem. Phys.* **1986**, *85*, 3975.

(24) Lucchese, B. R.; Schaefer, H. F. *J. Am. Chem. Soc.* **1978**, *100*, 298. Goddard, J. D.; Schaefer, H. F. *J. Chem. Phys.* **1979**, *70*, 5117.

(25) Flammang, R.; Haverbeke, Y. V.; Laurent, S.; Flammang, M.B.; Wong, M.W.; Wentrup, C. *J. Phys. Chem.* **1994**, *98*, 5801.

(26) Takumoto, T.; Saito, K.; Imamura, A. *J. Phys. Chem.* **1985**, *89*, 2286.